

Effects of Ni Thickness and Reflow Times on Interfacial Reactions between Ni/Cu Under-Bump Metallization and Eutectic Sn-Pb Solder in Flip-Chip Technology

CHIEN-SHENG HUANG,¹ JENQ-GONG DUH,^{1,4} YEN-MING CHEN,² and JYH-HWA WANG³

1.—Department of Materials Science and Engineering, National Tsing Hua University, Hsinchu, Taiwan. 2.—Department of Materials Science and Engineering, National Chiao Tung University, Hsinchu, Taiwan. 3.—Chunghwa Telecom Co., Ltd. Yang-Mei, Taoyuan, Taiwan. 4.—E-mail: jgd@mse.nthu.edu.tw

Flip-chip interconnection technology plays a key role in today's electronics packaging. Understanding the interfacial reactions between the solder and under-bump metallization (UBM) is, thus, essential. In this study, different thicknesses of electroplated Ni were used to evaluate the phase transformation between Ni/Cu under-bump metallurgy and eutectic Sn-Pb solder in the 63Sn-37Pb/Ni/Cu/Ti/Si₃N₄/Si multilayer structure for the flip-chip technology. Interfacial reaction products varied with reflow times. After the first reflow, layered (Ni_{1-x},Cu_x)₃Sn₄ was found between solder and Ni. However, there were two interfacial reaction products formed between solders and the UBM after three or more times reflow. The layered (Ni_{1-x},Cu_x)₃Sn₄ was next to the Ni/Cu UBM. The islandlike (Cu_{1-y},Ni_y)₆Sn₅ was formed between (Ni,Cu)₃Sn₄ and solders. The amounts of (Cu_{1-y},Ni_y)₆Sn₅ intermetallic compound (IMC) could be related to the Ni thickness and reflow times. In addition, the influence of Cu contents on phase transformation during reflow was also studied.

Key words: Flip chip, under-bump metallization, intermetallic compound, diffusion, phase transformation

INTRODUCTION

Flip-chip technology with the aid of ball-grid array interconnection has attracted a great amount of attention in today's electronics packaging. It provides many excellent advantages, such as a large number of input/output connections, good electrical performance, easy assembly, and high reliability.¹⁻³ One of the challenging issues is the material selection for under-bump metallization (UBM). Because of the rapid reaction of Sn with Cu, and the spalling effect of the Cu-Sn intermetallic compound (IMC), the Cu-based UBM has been found to be incompatible with SnPb solder or high melting-point solders.^{4,5} The Ni-based UBM is of interest in flip-chip technology because of the slower reaction rate with Sn in solder; thus, the spalling of the Ni-Sn compound will be limited.⁶

In the literature, most studies were focused on

solders with Ni-based UBM during liquid-state annealing, i.e., annealing above the melting point for several minutes or hours.⁷⁻¹¹ However, the dwelling time, i.e., the total time of temperature above the melting point for real reflow process is less than 100 sec. That is to say, the associated reaction between liquid-state annealing and soldering reflow should be quite different, owing to the distinction of time duration. It is, thus, interesting to evaluate the interfacial reaction between PbSn solder and Ni/Cu UBM during multiple reflows. In this study, a 63Sn-37Pb/Ni/Cu/Ti/Si₃N₄/Si multilayer structure was used. Titanium played the role of the adhesion layer, and Cu was the conductor, while Ni acted as the wetting layer and the diffusion barrier. Different thicknesses of Ni (1 μm, 3 μm, 5 μm, 6 μm, and 9 μm) and multiple reflow (1, 3, and 5 times) were carried out. According to the compositions of IMCs evaluated in the joint, the phenomenon of phase transformation during soldering reflow could be studied.

(Received July 19, 2002; accepted August 28, 2002)

EXPERIMENTAL PROCEDURE

Figure 1 shows the UBM structure used in this study. The top metal of the Si wafer was Cu, which acted as an interconnection line. The adhesion layer was sputtered Ti of 1,000 Å. Then, 5,000-Å Cu was sputtered on Ti for electroplating seed layer. The electroplated Cu was further deposited on the metallized substrate. The thickness of the electroplated Cu was 5 μm. Nickel with different thicknesses was electroplated on the top of the electroplated Cu. The thicknesses of Ni selected in this study were 1 μm, 3 μm, 5 μm, 6 μm, and 9 μm. After UBM was plated onto a Si wafer, the eutectic Sn-Pb solder bump was then electroplated. All metal films were deposited consecutively without breaking vacuum.

Solder reflows were conducted in an infrared solder-reflow oven. The peak temperature and dwelling time of the reflow profile were 225°C and 70 sec, respectively. The cycles of solder reflow were one to five.

The surface morphology of electroplated Ni was characterized by an atomic force microscope. The interfacial morphologies between Sn-Pb solder and UBM were analyzed with a scanning electron microscope. The compositions of phases in the solder joints and elemental distribution across the joint interface were quantitatively measured with an electron probe microanalyzer (EPMA) with the aid of the ZAF correction program.¹²

RESULTS AND DISCUSSION

Interfacial Reaction between PbSn Solder and Ni/Cu UBM

Cross-sectional images of the Pb-Sn solder/Ni interface after one reflow are shown in Fig. 2. The thicknesses of Ni were 1 μm, 3 μm, 5 μm, 6 μm, and 9 μm, respectively. Only one layer of IMC was found between solder and Ni in all joints after one

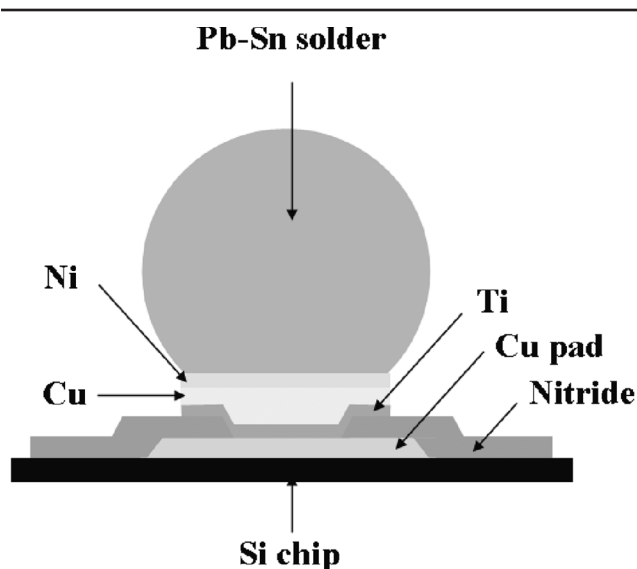
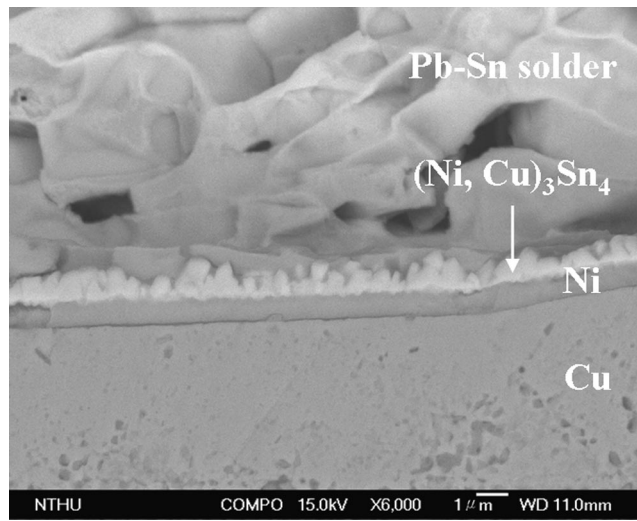


Fig. 1. The schematic illustration of UBM.

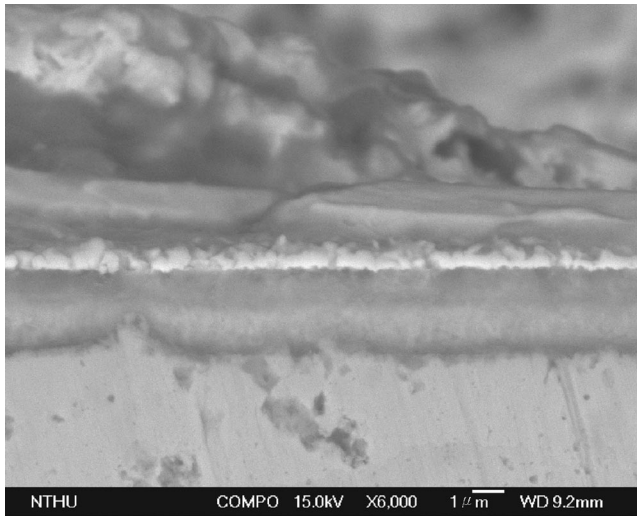
reflow. The reacted layer was less than 1 μm. In the case of 1-μm Ni, the composition of the reaction product was 57.5at.%Sn-36.4at.%Ni-6.1at.%Cu. The IMC size is close to the detection limit of the EPMA if the resolution of electron probe size is considered. To obtain the quantitative data more precisely, a detailed and deliberative task was carried out in the EPMA analysis by controlling the appropriate accelerating voltage, beam current, and focus-beam size. The reported compositions as listed in this study were, in fact, the average of at least 10 measured points. The ratio of the atomic percentage of (Ni + Cu) to Sn was (36.4 + 6.1): (57.5), which is close to 3:4. Thus, this IMC could be denoted as $(\text{Ni}_{1-x}, \text{Cu}_x)_3\text{Sn}_4$. A similar observation was reported recently in the literature,¹³⁻¹⁵ yet the concentrations of Cu in Ni_3Sn_4 were all different. In the other cases of different Ni thicknesses (3 μm, 5 μm, 6 μm, and 9 μm), the reaction products were also identified as $(\text{Ni}_{1-x}, \text{Cu}_x)_3\text{Sn}_4$. However, the values of x in $(\text{Ni}_{1-x}, \text{Cu}_x)_3\text{Sn}_4$ were different, as represented in Fig. 3 after detailed composition analysis by EPMA. As the thickness of Ni increased, the values of x in $(\text{Ni}_{1-x}, \text{Cu}_x)_3\text{Sn}_4$ decreased. The formation of $(\text{Ni}_{1-x}, \text{Cu}_x)_3\text{Sn}_4$ implied that Cu diffused through Ni and reacted with Ni and Sn, even for the case with 9-μm Ni.

Figure 4 represents the cross-sectional images of the Pb-Sn solder/Ni interface after three reflow times. There were two types of IMCs found between solders and electroplated Ni. One was a layered type, and the other was island type. The thickness of the layered-type IMC was still less than 1 μm, and the diameter of the island type was about 1 μm. The layered-type IMC was identified as $(\text{Ni}_{1-x}, \text{Cu}_x)_3\text{Sn}_4$ with the aid of EPMA quantitative analysis. The composition of the island-type IMC was 44.8at.%Sn-33.1at.%Cu-22.1at.%Ni. The ratio of the (Cu + Ni) to Sn was close to 6:5. Thus, this IMC could be considered as $(\text{Cu}_{1-y}, \text{Ni}_y)_6\text{Sn}_5$. The amount of $(\text{Cu}_{1-y}, \text{Ni}_y)_6\text{Sn}_5$ formed was different in samples of different Ni thickness. As the thickness of the Ni increased, the amount of $(\text{Cu}_{1-y}, \text{Ni}_y)_6\text{Sn}_5$ decreased. Statistically speaking, at least one $(\text{Cu}_{1-y}, \text{Ni}_y)_6\text{Sn}_5$ IMC could be found in the joint with 1-μm Ni. There was nearly one $(\text{Cu}_{1-y}, \text{Ni}_y)_6\text{Sn}_5$ IMC found in the joint with 3-μm Ni. Nevertheless, in the case of joints with 9-μm Ni, the probability to observe one IMC was around 30%. In fact, this could be related to the Cu contents in $(\text{Ni}_{1-x}, \text{Cu}_x)_3\text{Sn}_4$.

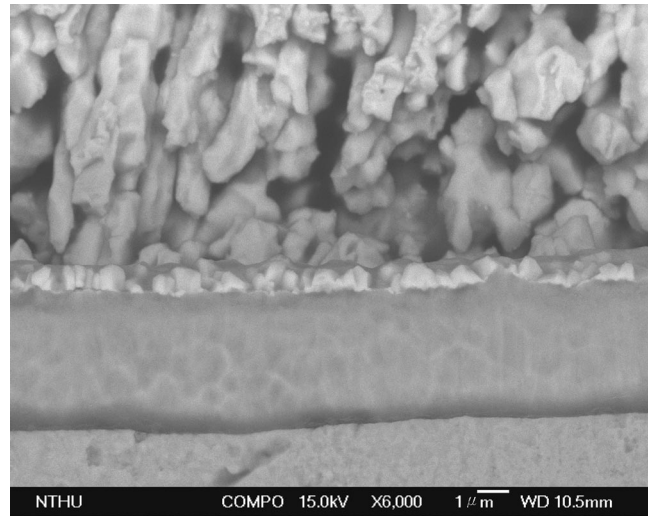
For the Pb-Sn solder/Ni interface after five times reflow, the interfacial morphology was very similar to that after three reflow times. Both layered type $(\text{Ni}_{1-x}, \text{Cu}_x)_3\text{Sn}_4$ and island-type $(\text{Cu}_{1-y}, \text{Ni}_y)_6\text{Sn}_5$ were formed between PbSn solder and Ni. The only difference was the quantities of $(\text{Cu}_{1-y}, \text{Ni}_y)_6\text{Sn}_5$. With increasing reflow times, the amounts of $(\text{Ni}_{1-x}, \text{Cu}_x)_3\text{Sn}_4$ increased. For example, in the case of 9-μm Ni, at least one $(\text{Cu}_{1-y}, \text{Ni}_y)_6\text{Sn}_5$ IMC could be found in the interface of each solder joint.



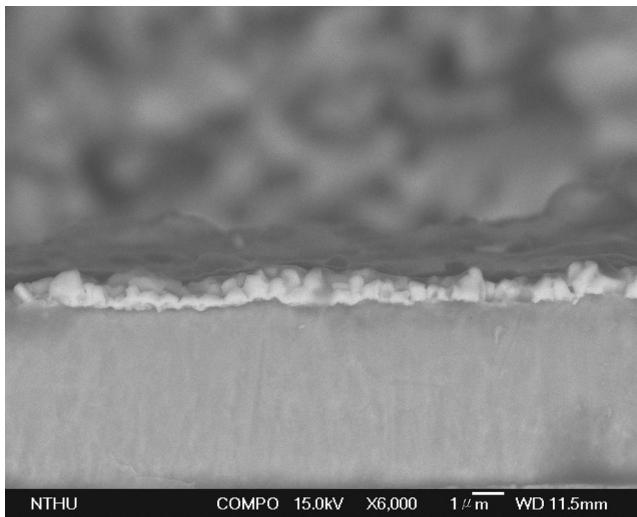
a



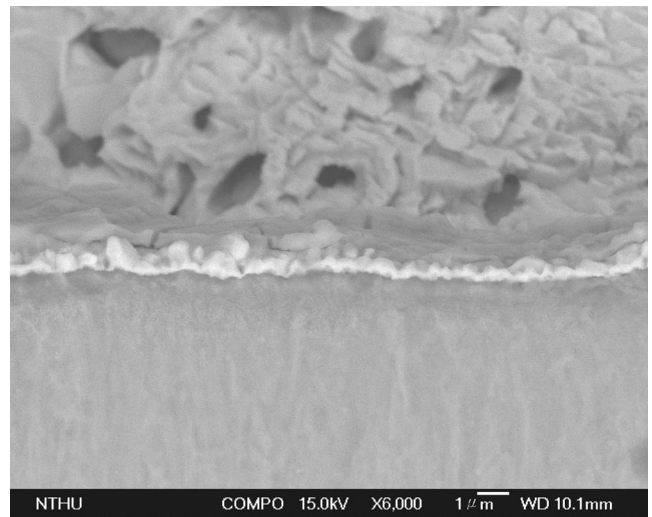
b



c



d



e

Fig. 2. The cross-sectional images of solder/UBM interfaces after one reflow: (a) 1- μ m Ni, (b) 3- μ m Ni, (c) 5- μ m Ni, (d) 6- μ m Ni, and (e) 9- μ m Ni.

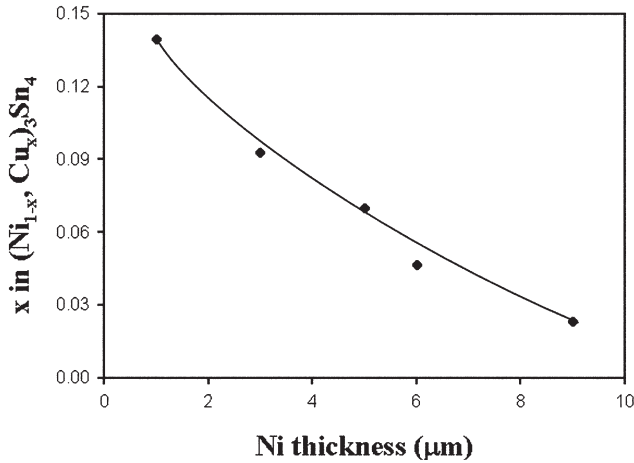


Fig. 3. The values of x in $(\text{Ni}_{1-x}, \text{Cu}_x)_3\text{Sn}_4$ as a function of Ni thickness.

Phase Transformation during Reflow

To investigate the phase transformation during the first and the third cycle of reflow, the compositions in the $(\text{Ni}_{1-x}, \text{Cu}_x)_3\text{Sn}_4$ IMC near the $(\text{Cu}_{1-y}, \text{Ni}_y)_6\text{Sn}_5$ IMC were further investigated. Figure 5 shows the interfacial microstructure between the Sn-Pb solder/ $1\text{-}\mu\text{m}$ Ni after three reflows. In this figure, three trace points, i.e., one far away from $(\text{Cu}_{1-y}, \text{Ni}_y)_6\text{Sn}_5$; another near $(\text{Cu}_{1-y}, \text{Ni}_y)_6\text{Sn}_5$, and the other very close to $(\text{Cu}_{1-y}, \text{Ni}_y)_6\text{Sn}_5$, were denoted as A, B, and C, respectively. After detailed quantitative analysis by EPMA, the compositions of point A, B, and C are listed in Table I. For the trace point far away from $(\text{Cu}_{1-y}, \text{Ni}_y)_6\text{Sn}_5$, the compositions of $(\text{Ni}_{1-x}, \text{Cu}_x)_3\text{Sn}_4$ were very close to that in the as-reflowed case. However, with the trace position close to the $(\text{Cu}_{1-y}, \text{Ni}_y)_6\text{Sn}_5$ IMC, Cu contents in $(\text{Ni}_{1-x}, \text{Cu}_x)_3\text{Sn}_4$ increased. This implies that the amount of Cu dissolution in $(\text{Ni}_{1-x}, \text{Cu}_x)_3\text{Sn}_4$ increased.

The composition of $(\text{Cu}_{1-y}, \text{Ni}_y)_6\text{Sn}_5$ was identical in all joints. That is to say, the value of y in $(\text{Cu}_{1-y}, \text{Ni}_y)_6\text{Sn}_5$ remains constant. However, the value of x in $(\text{Ni}_{1-x}, \text{Cu}_x)_3\text{Sn}_4$ is not fixed. As described previously, x varied from 0.14 to 0.35 in the case of $1\text{-}\mu\text{m}$ Ni. In the cases of $3\text{-}\mu\text{m}$, $5\text{-}\mu\text{m}$, $6\text{-}\mu\text{m}$, and $9\text{-}\mu\text{m}$ Ni, the values of x in $(\text{Ni}_{1-x}, \text{Cu}_x)_3\text{Sn}_4$ varied from 0.09 to 0.35, 0.07 to 0.35, 0.05 to 0.35, and 0.02 to 0.35, respectively, again after deliberative EPMA analysis. Variations of x might be related to IMCs phase transformation in the consideration of ternary Ni-Cu-Sn phase equilibrium. A further investigation concerning this aspect is currently under way and will be reported in a future paper.

As mentioned previously, Cu diffused through electroplated Ni and reacted with Ni along the passage, and then reacted with Sn from the solder to form $(\text{Ni}_{1-x}, \text{Cu}_x)_3\text{Sn}_4$ after one reflow. Thus, the x value in $(\text{Ni}_{1-x}, \text{Cu}_x)_3\text{Sn}_4$ corresponded to the amount of diffused Cu. With the increasing thickness of Ni, the amount of Cu diffused should decrease. During the third cycle of reflow, the diffused Cu might dissolve into $(\text{Ni}_{1-x}, \text{Cu}_x)_3\text{Sn}_4$ to form $(\text{Ni}_{1-z},$

Table I. Compositions of Trace Points A, B, and C in Figure 5

Position	Composition (at.%)		
	Sn	Ni	Cu
A	57.5	36.4	6.1
B	57.1	34.0	8.9
C	56.9	27.9	15.2

$\text{Cu}_z)_3\text{Sn}_4$, where z indicates the maximum solubility of Cu in Ni_3Sn_4 . After Ni_3Sn_4 reached its maximum solubility of Cu, the excess Cu continued to diffuse through $(\text{Ni}_{1-z}, \text{Cu}_z)_3\text{Sn}_4$ into the solder. The excess Cu then reacted with Ni and Sn to form $(\text{Cu}_{1-y}, \text{Ni}_y)_6\text{Sn}_5$. It should be pointed out that the growth of Ni_3Sn_4 was limited during reflow, as shown in Figs. 2 and 4. Thus, Cu could dissolve and diffuse through Ni_3Sn_4 easier. However, this phenomenon did not occur everywhere. In general, the $(\text{Cu}_{1-y}, \text{Ni}_y)_6\text{Sn}_5$ IMC was first observed near the edge of solder joints.

Cu Diffusion through Ni

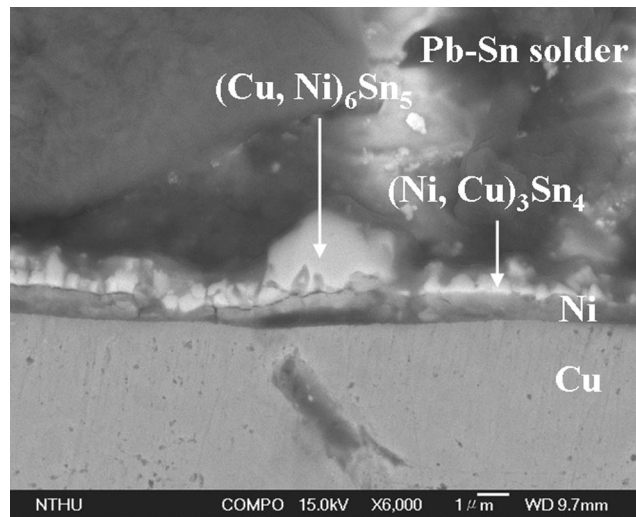
The presence of Cu in Ni_3Sn_4 implies that Cu might diffuse through Ni and substitute for the Ni sites. The surface morphology of $3\text{-}\mu\text{m}$ Ni analyzed with an atomic force microscope is shown in Fig. 6, which indicates that the electroplated Ni exhibits a columnar structure. The Cu could move through the column boundary to enhance its diffusivity. With increasing thickness of Ni, the pathway for Cu atoms diffusion was prolonged. As a result, the degree of Cu migration through Ni was retarded and, thus, the x value in $(\text{Ni}_{1-x}, \text{Cu}_x)_3\text{Sn}_4$ was decreased, as observed in the EPMA result. A further study concerning the diffusion behavior of Cu in this joint assembly will be reported in the near future.

CONCLUSIONS

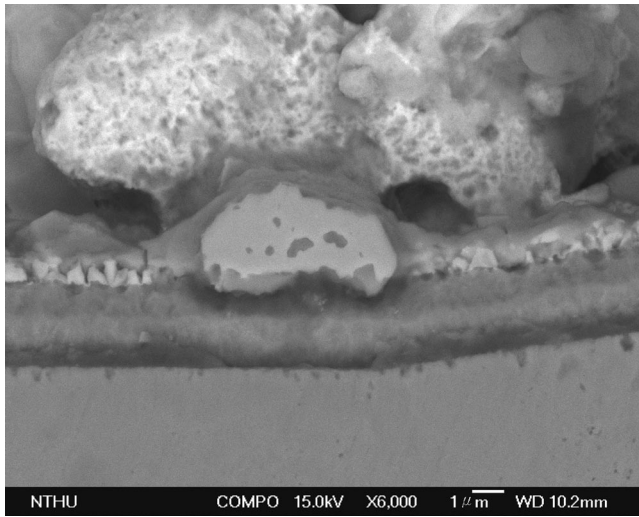
After one reflow, only one layer of $(\text{Ni}_{1-x}, \text{Cu}_x)_3\text{Sn}_4$ was found between solders and electroplated Ni in joints of a $63\text{Sn-}37\text{Pb/Ni/Cu/Ti/Si}_3\text{N}_4/\text{Si}$ multilayer structure. As the thickness of Ni increased, the values of x in $(\text{Ni}_{1-x}, \text{Cu}_x)_3\text{Sn}_4$ decreased. Both layered $(\text{Ni}_{1-x}, \text{Cu}_x)_3\text{Sn}_4$ and island-type $(\text{Cu}_{1-y}, \text{Ni}_y)_6\text{Sn}_5$ were found between solders and electroplated Ni in all joints after three or five reflow times. When the thickness of Ni increased, the quantity of $(\text{Cu}_{1-y}, \text{Ni}_y)_6\text{Sn}_5$ decreased. However, with increasing reflow times, the quantities of $(\text{Cu}_{1-y}, \text{Ni}_y)_6\text{Sn}_5$ increased. After several reflows, Cu first diffused through electroplated Ni and reacted with Ni and Sn to form $(\text{Ni}_{1-x}, \text{Cu}_x)_3\text{Sn}_4$. The Ni_3Sn_4 would then reach its maximum solubility of Cu. Eventually, the excess Cu and Ni further migrated into solders to form $(\text{Cu}_{1-y}, \text{Ni}_y)_6\text{Sn}_5$.

ACKNOWLEDGEMENTS

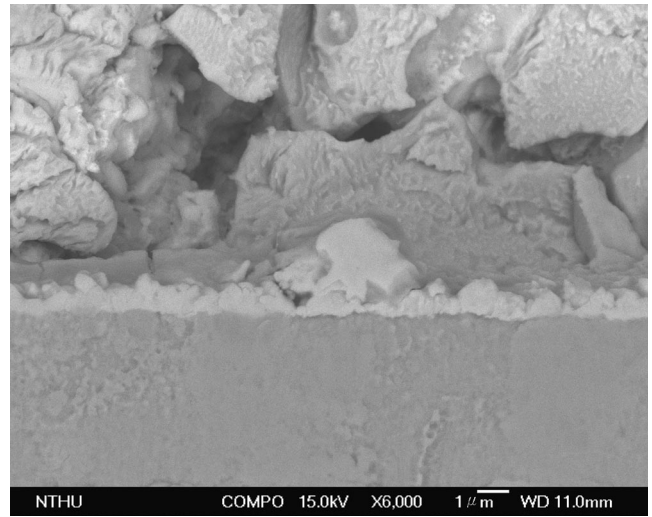
The financial support from Taiwan Semiconductor Manufacturing Company is acknowledged. Par-



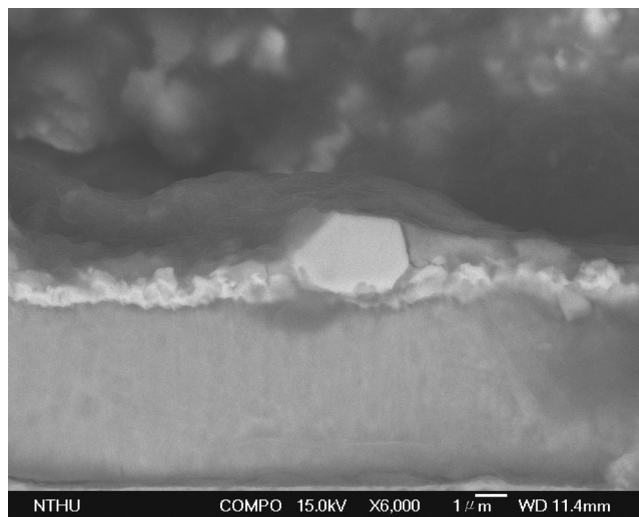
a



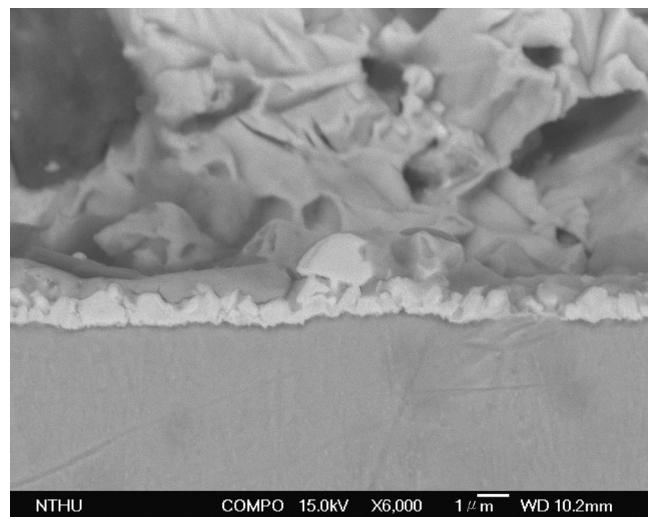
b



c



d



e

Fig. 4. The cross-sectional images of solder/UBM interfaces after three reflow times: (a) 1- μm Ni, (b) 3- μm Ni, (c) 5- μm Ni, (d) 6- μm Ni, and (e) 9- μm Ni.

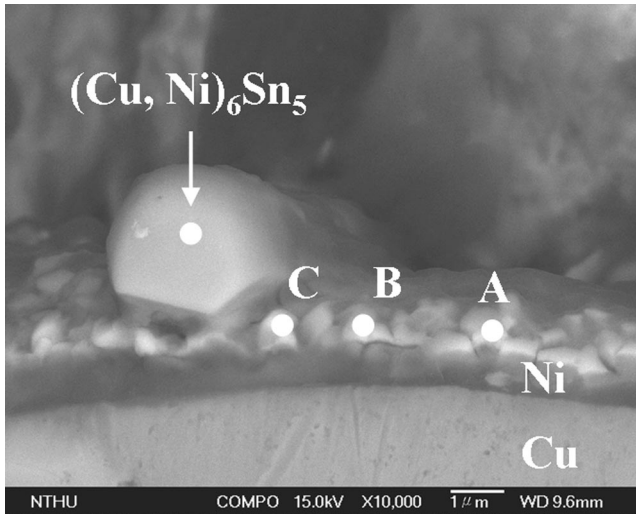


Fig. 5. The interfacial microstructure between Sn-Pb solder/1- μm Ni after three reflow times. Point A: far away from $(\text{Cu}, \text{Ni})_6\text{Sn}_5$; point B: near $(\text{Cu}, \text{Ni})_6\text{Sn}_5$; and point C: very close to $(\text{Cu}, \text{Ni})_6\text{Sn}_5$.

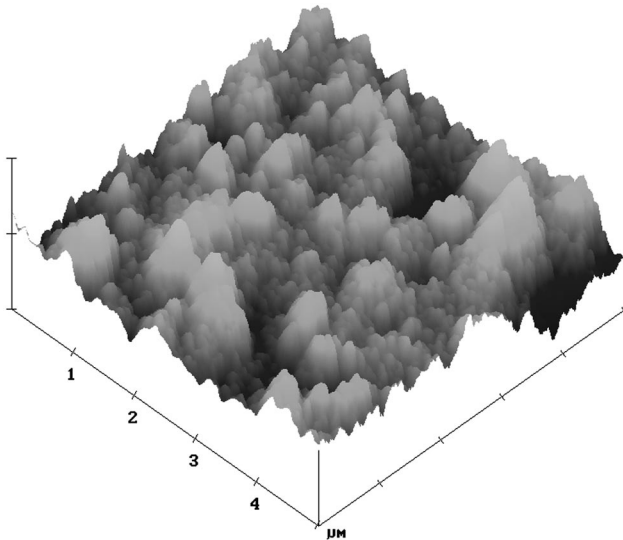


Fig. 6. The surface morphology of as-deposited 3- μm Ni film.

tial support from the National Science Council under Contract No. NSC-90-2216-E007-058 is also acknowledged.

REFERENCES

1. J.H. Lau, *Flip Chip Technologies* (New York: McGraw-Hill, 1996).
2. C.S. Chang, A. Oscilowski, and R.C. Bracken, *IEEE Circ. Dev. Mag.* 14, 45 (1998).
3. D.S. Patterson, P. Eleniu, and J.A. Leal, *Adv. Electron. Packaging* 1, 337 (1997).
4. A.A. Liu, H.K. Kim, K.N. Tu, and P.A. Totta, *J. Appl. Phys.* 80, 2774 (1996).
5. H.K. Kim, K.N. Tu, and P.A. Totta, *Appl. Phys. Lett.* 68, 2204 (1996).
6. D.R. Frear, F.M. Hosking, and P.T. Vianco, *Materials Developments in Microelectronic Packaging Conf. Proc.*, ed. P. Singh (Materials Park, OH: ASM International, 1991), pp. 229–239.
7. S. Bader, W. Gust, and H. Hieber, *Acta Metall. Mater.* 43, 329 (1995).
8. S.K. Kang, R.S. Raiand, and S. Purushothaman, *J. Electron. Mater.* 25, 1113 (1996).
9. C.E. Ho, Y.M. Chen, and C.R. Kao, *J. Electron. Mater.* 28, 1231 (1999).
10. P.G. Kim, J.W. Wang, T.Y. Lee, and K.N. Tu, *J. Appl. Phys.* 86, 6746 (1999).
11. T.M. Korhonen, P. Su, S.J. Hong, M.A. Korhonen, and C.Y. Li, *J. Electron. Mater.* 28, 1146 (1999).
12. J.I. Goldstein, *Scanning Electron Microscopy and X-ray Microanalysis* (New York: Plenum Press, 1981).
13. B.L. Young and J.G. Duh, *J. Electron. Mater.* 30, 878 (2001).
14. G. Ghosh, *Acta Mater.* 48, 3719 (2000).
15. J.Y. Park, C.W. Yang, J.S. Ha, C.U. Kim, E.J. Kwon, S.B. Jung, and C.S. Kang, *J. Electron. Mater.* 30, 1165 (2001).